STIC-ILL

From: Afremova, Vera
Sent: Wednesday, April 23, 2003 2:43 PM
To: STIC-ILL
Subject: 10/032,728

Hi, please, could I have this ref.:

Laughlin et al. Am. J. Physiol. 1993. 264:H2068-H2079.

Vera Afremova
CM1 11E13
308-9351

Pyruvate and lactate metabolism in the in vivo dog heart

MAREN R. LAUGHLIN, JONI TAYLOR, A. SCOTT CHESNICK,
MICHAEL DEGROOT, AND ROBERT S. BALABAN
Laboratory of Cardiac Energetics, National Heart, Lung, and Blood Institute, National Institutes of Health, Bethesda, Maryland 20892

Laughlin, Maren R., Joni Taylor, A. Scott Chesnick, Michael DeGroot, and Robert S. Balaban. Pyruvate and lactate metabolism in the in vivo dog heart. *Am. J. Physiol.* 264 (*Heart Circ. Physiol.* 33): H2068-H2079, 1993.—Pyruvate increases the phosphorylation potential in perfused heart to a greater extent than the closely correlated substrate L-lactate. Therefore, metabolism of these compounds was studied in the myocardium of intact dogs. Phosphocreatine/ATP was increased 23% at 5.3 mM plasma pyruvate but was not significantly increased by lactate except at the highest concentration (17.5 mM in blood). Calculated [ADP] fell during pyruvate infusion from 51.5 ± 2.0 to 38.6 ± 3.3 μM but did not change significantly during lactate infusion. Intracellular free [Mg^{2+}] fell from 705 ± 53 to 498 ± 30 μM at the highest pyruvate infusion and from 602 ± 112 to 417 ± 19 μM with lactate infusion. Extraction of both substrates was linear at low concentrations, reaching 0.56 μmol lactate·min^{-1}· g wet wt^{-1} at 17.5 mM blood lactate and 0.58 μmol pyruvate·min^{-1}·g wet wt^{-1} at 5.3 mM plasma pyruvate. Therefore, lactate uptake was almost five times lower than pyruvate uptake at similar concentrations. Elevated pyruvate (>3 mM) resulted in almost complete inhibition of net lactate uptake. Infused [3-^{13}C]lactate or -pyruvate gave rise to labeled glutamate and alanine in vivo, but labeled lactate was not visible when [3-^{13}C]pyruvate was the substrate. The ^{13}C enrichment of myocardial lactate was similar to alanine and acetyl CoA with infused [3-^{13}C]lactate but was only one-half that of alanine and acetyl CoA when [3-^{13}C]-pyruvate was the substrate, indicating a possible inhibition of lactate dehydrogenase.

oxygen consumption; redox potential; myocardial metabolism; phosphorus-31 nuclear magnetic resonance; carbon-13 nuclear magnetic resonance; phosphocreatine; phosphorylation potential; adenosine 5'-triphosphate; magnesium; glutamate; alanine; intracellular pH

IT HAS BEEN SHOWN that many substrates, when provided to the perfused heart, can dramatically raise the resting phosphorylation potential (3, 14, 28, 43, 50) as well as alter the response of the phosphorylation potential to work (3, 9, 50). These compounds include acetate, fatty acids, and pyruvate. Recent studies have also demonstrated that this can occur in vivo with elevated β-hydroxybutyrate (21). This work raises the possibility of a relationship between the utilization of different substrates and the regulation of oxidative phosphorylation in vivo (17).

Because of the complexity of both the in vivo model and intracellular substrate metabolism, we have chosen to compare the effects of two related compounds, lactate and pyruvate. Pyruvate and lactate both enter the trichloroacetic acid (TCA) cycle through pyruvate dehydrogenase (PDH), yet pyruvate has been shown to have a larger effect on the phosphorylation potential in the perfused heart (3, 28, 50). Of these two substrates, lactate is the physiological source of reducing equivalents (7, 12). Its extraction is proportional to the circulating concentration and provides ≤25% of substrate for oxidation at normal physiological levels (~0.5 mM; see Refs. 7, 25). At elevated concentrations, even those that occur during heavy exercise in humans, the heart is able to obtain 60-90% of its oxidizable carbon source from lactate (1, 7, 20). Pyruvate is an oxidized form of lactate, and the two compounds actually enter the heart cell through the same pH-dependent monocarboxylate transporter (37, 44, 45). In isolated cardiac myocytes, pyruvate and lactate have a similar maximum velocity of uptake (V_{max}; 2.7 vs. 1.9 nmol·min^{-1}·μl intracellular $space^{-1}$), but pyruvate has the greater affinity for the transporter [Michaelis constant (K_m) = 70 μM for pyruvate vs. 2.3 mM for L-lactate; see Ref. 37]. The trend is similar in cardiac sarcolemmal vesicles, where the K_m for lactate transport is ~27 vs. ~5.0 mM for pyruvate (37, 44). Once inside, pyruvate can be used directly by the mitochondria, whereas lactate is readily converted to pyruvate by the heart isozyme of lactate dehydrogenase (LDH), which has an activity of 5,574 U/g dry wt and is thought to be near equilibrium (38).

A further advantage of comparing the effects of lactate and pyruvate on energy production in vivo is that their ^{13}C-nuclear magnetic resonance (NMR) profiles were measured by Sherry et al. (41) in perfused heart and can be compared with the spectra taken in vivo. Perfusion with ^{13}C-labeled pyruvate gives rise to labeled glutamate, aspartate, alanine, citrate, malate, lactate, and acetylcarnitine, whereas [3-^{13}C]lactate perfusion results primarily in labeled glutamate. The reasons for the differences in these labeling patterns may be due to cytosolic NADH production and malate-aspartate shuttle activity.

The purpose of this study was therefore to evaluate the different effects of lactate and pyruvate on energy metabolism in the in vivo canine heart under normal substrate conditions using ^{31}P- and ^{13}C-NMR and organ balance techniques.

METHODS

Animal preparation. Twenty-three female beagles (body wt 26.5 ± 0.9 lb.) that had been fasted overnight were surgically prepared essentially as previously described (21, 25). They were sedated with 20 mg/kg iv thiopental sodium, intubated, and ventilated with 50% O_2-0.8% halothane-N_2 using a servo-pediatric ventilator (Siemens-Elema AB 900D, Solna, Sweden). A cannula was placed in a carotid artery and attached to a nonmagnetic transducer (Cobe Laboratories, Lakewood, CO) for monitoring blood pressure and heart rate. Arterial blood samples were drawn for blood gases. A second catheter was placed in the left external jugular for infusion of substrates and Ringer solution to maintain hydration. Potassium and bicarbonate were added as needed. A bipolar pacing lead was inserted into the right atrium via the right external jugular vein. A median sternotomy allowed exposure of the heart, and pericardial fat was removed by blunt dissection and cautery.

In the eight dogs used for ^{31}P-NMR and myocardial extraction measurements, a coronary sinus-venous shunt was placed so that the arterial-venous difference of O_2, glucose, lactate, and pyruvate could be measured (see Refs. 21, 25 for details). One end was securely inserted into the coronary sinus through the right atrium and the other into the right external jugular vein to return the blood to the circulation. Heparin solution was dripped through the shunt to prevent clot formation. The shunt included a flow probe (Transonics Systems, Ithaca, NY) and a stopcock for venous blood sampling. Arterial blood samples were drawn from the carotid artery. At the end of the experiment, the left ventricle was dissected away from the rest of the heart, blotted dry, and weighed.

In ^{13}C-NMR tracer experiments, a small branch off of the left anterior descending artery (LAD) was isolated near the base of the heart and cannulated in a retrograde direction for the local infusion of tracer to the left ventricle as was previously described (25). A heparinized solution was infused continuously at 30 ml/h to prevent clotting of this catheter. In two dogs, another catheter was placed in a vein on the anterior surface of the heart to measure ^{13}C enrichment in the venous drainage from the apex during infusion of ^{13}C-labeled substrate into the LAD.

For NMR experiments, a 2-cm surface receiver coil was sutured to the pericardium over the apex, and the probe body was secured in place on styrofoam blocks that also served to spread the ribs. The chest was protected against heat and water loss with plastic wrap, and the entire animal was wrapped in a space blanket (Boy Scouts of America, Charlotte, NC) and placed on a warmed circulating water blanket.

Chemical analysis. Blood pH and ion concentrations were measured with a Ciba-Corning 288 blood gas system (Ciba-Corning Diagnostics, Medfield, MA), which also estimated hematocrit using the following formula: hematocrit = total hemoglobin × 2.941. O_2 content was measured using an associated 2500 CO-oximeter (Ciba-Corning Diagnostics). Glucose and L-lactate in whole blood were measured with a Yellow Springs 2300 STAT glucose/lactate analyzer (Yellow Springs, OH). For the chemical analysis of pyruvate and alanine, heparinized blood was immediately centrifuged and the plasma was extracted with 2 vol of cold 6% perchloric acid. Standard enzyme-linked assays were performed (2, 36).

Protocols. The following general protocol was followed for all experiments. After a basal period of 20–30 min, sodium-L-lactate or sodium-pyruvate was freshly made in sterile water (pH 6.0–6.5) and infused into the animals while measurements were made. The tidal volume and O_2 concentration in the inspired air were originally adjusted to give an arterial pH of ~7.33. This was done because of the tendency of the pH to drift upward during systemic pyruvate or lactate infusion (4). Care was taken to maintain the arterial pH below 7.5 throughout the experiment and to correct arterial potassium, calcium, and magnesium.

Phosphorus-31 NMR and substrate extraction. After a 30-min control period in which basal ^{31}P-NMR spectra and two extraction measurements were made, 600 mM L-lactate or pyruvate (Sigma, St. Louis, MO) was infused at different rates for 30 min at each rate. Blood samples were removed from the carotid artery and the coronary sinus every 15 min for extraction measurements of glucose, lactate, and O_2 and every 30 min near the end of each infusion period for measurement of pyruvate. Pyruvate experiments had infusion rates of 30, 60, 120, and 180 ml/h, and lactate experiments had rates of 60, 120, 180, and 240 ml/h. The ^{31}P NMR spectra were taken throughout.

Carbon-13 NMR tracer experiments. After five basal ^{13}C NMR spectra (22.5 min), an infusion of Na-L-[3-^{13}C]lactate (n = 4) or Na[3-^{13}C]pyruvate (n = 4) (MSD Isotopes, St. Louis, MO; 0.10 mmol/min) was started into the LAD catheter, and spectra were acquired for an additional 70 min. Insulin (40 mU/min) was infused into the jugular vein to maximize carbohydrate metabolism, along with a variable glucose drip to prevent hypoglycemia. An additional three dogs were used to evaluate the effects of elevated pyruvate on the metabolism of labeled lactate. Either a tubing shunt was placed in the coronary sinus as above or a catheter was positioned in the coronary sinus through the right jugular vein. Unlabeled pyruvate was infused into the left jugular vein in graded doses until lactate uptake (as measured from arterial-coronary sinus differences) returned to its basal level or below (<0.02 μmol·min^{-1}·g wet wt^{-1}). The pyruvate infusion was continued at this rate while 0.10 mmol/min [3-^{13}C]lactate was infused into the LAD for 45 min and ^{13}C-NMR spectra were acquired.

In three experiments from each group, dogs were removed from the magnet, and 1–2 g of tissue from the apex were freeze clamped in situ while the labeled infusion continued. Care was taken to avoid or to remove excess blood from the cardiac chambers in these samples. The tissue was homogenized using a Virtishear homogenizer (Virtis, Gardiner, NY) in 10–20 vol 6% perchloric acid neutralized with 5 M KOH and lyophilized. Extracts were reconstituted in a 100 mM phosphate buffer, pH 7.17, made in D_2O (99.9%, MSD Isotopes), and used for proton and carbon NMR analysis.

Label exchange. LAD and venous catheters were placed in the anterior surface of the left ventricle in two dogs. The [3-^{13}C]lactate and unlabeled pyruvate were infused together into the LAD at a rate of 0.10 mmol/min for 40 min. Venous blood samples were drawn at 15 and 35 min, and the heart was freeze clamped at 40 min. After blood glucose and lactate were measured, the blood was immediately extracted with one-half volume of cold 18% perchloric acid. The precipitated protein was centrifuged away, and the acidic supernatant was immediately examined with proton NMR for lactate and pyruvate ^{13}C enrichment.

NMR measurements. All in vivo NMR experiments were performed using a General Electric spectrometer (Freemont, CA) equipped with a 4.7-tesla, 26-cm bore horizontal magnet (Oxford Instruments, Oxford, UK). For ^{31}P-NMR experiments, the two-turn, 2-cm diam surface coil was tuned to 81.011 MHz (21). For ^{13}C-NMR experiments, the probe contained two concentric surface coils. The inner two-turn, 2-cm inductor was tuned to 50.32 MHz for carbon excitation, and the outer 4-cm copper foil coil was tuned to 200.12 MHz for proton decoupling and nuclear Overhauser effect (NOE) development (25). Shimming of the water resonance (35–50 Hz for ^{31}P experiments, 60–90 Hz for ^{13}C experiments) was achieved during gating of the spectrometer to the respirator while the heart was paced to a harmonic of the respirator rate. The difference in homogeneity was due to signal acquired from the chest wall by the large proton coil in the ^{13}C-NMR experiments. The gating pulse was generated using an in-house program running on a DEC MINC-11 computer (Digital Equipment, Merrimack, NH).

Phosphorus and carbon spectra each consisted of 128 transients that were gated to the respirator (2-s interpulse delays). The pulse width was optimized at this repetition rate on the PCr peak for ^{31}P spectra and on the large fat peak at 30 ppm for ^{13}C spectra (usually 80 μs for each). In ^{13}C spectra, proton decoupling (MLEV64, 30 W) was used during acquisition, and NOE development was produced during relaxation with low power (2–3 W). A control spectrum was subtracted from each experimental spectrum. For both ^{13}C and ^{31}P experiments, 2–3 free induction decays were routinely combined to increase the signal-to-noise ratio. The spectra were then zero filled and processed with 10–20 Hz of exponential line broadening. Peak areas for all spectra were determined by integration.

Spectra of extracts were taken on a Bruker AC-300 (Bruker Instruments, Wilmington, DE) using a commercial 5-mm

broadband probe. Proton spectra consisted of 32 or 64 transients using 90° pulses and 10-s interpulse delays. Proton-decoupled ^{13}C spectra were acquired without NOE development using 90° pulses and 20-s delays (1,280–2,560 transients). These were zero filled and exponentially broadened. Areas were determined by integration in the proton spectra and by Lorenzian peak fitting in the ^{13}C spectra (GLINFIT software, A. D. Bain, Bruker Spectrospin Canada).

Calculation of intracellular free [Mg^{2+}] and [ADP]. Free [Mg^{2+}] was determined from the chemical shifts of α- and β-ATP in the in vivo ^{31}P-NMR spectra using the following equation

$$[Mg^{2+}] = K_D(\text{Mg-ATP}) \times \frac{\delta_{\alpha\beta}\text{ATP} - \delta_{\alpha\beta}}{\delta_{\alpha\beta} - \delta_{\alpha\beta}\text{Mg-ATP}}$$

where the Mg-ATP dissociation constant [K_D(Mg-ATP)] = 0.045 mM, $\delta_{\alpha\beta}$ is the chemical shift difference between the ^{31}P-NMR α- and β-ATP peaks, and $\delta_{\alpha\beta}$Mg-ATP = 8.31 and $\delta_{\alpha\beta}$ATP = 10.93 are the shift differences when Mg^{2+} is saturating and absent, respectively (15). Free [Mg^{2+}] was also determined from the chemical shift of the methylene carbons of citrate in ^{13}C-NMR spectra whenever this compound was visible ($n = 4$) using a similar equation, where K_D(Mg-citrate) = 0.46 mM and the chemical shifts of Mg^{2+}-citrate and Mg^{2+}-free citrate are 44.95 and 46.82 ppm, respectively (5). [ADP] could then be calculated from the PCr kinase equilibrium constant (K_{eq}), which is dependent on both intracellular pH and free [Mg^{2+}]. The following equation was used

$$[\text{ADP}] = \frac{[\text{ATP}] \times [\text{Cr}]}{K_{eq}(Mg^{2+}, \text{pH}) \times [\text{PCr}]}$$

where $K_{eq}(Mg^{2+},\text{pH})$ was calculated from equations in Ref. 26 and the control values for [PCr]/[ATP] (1.9), [ATP] (6.6 mM), and total creatine (27.3 mM) were taken from Ref. 16.

Calculation of ^{13}C enrichments from extract spectra. The enrichment of alanine and lactate, as well as the ratio of total alanine to lactate, was determined from proton spectra of heart extracts. The protons bound to an unlabeled methyl carbon appear as a doublet. Those bound to a ^{13}C (one-half spin) are split into two pairs of peaks that resonate on either side of the central doublet, with a J coupling of 128 Hz. The enrichment with ^{13}C is the ratio of the area of the two side peaks to the combined area of the central and side peaks. The ^{13}C enrichment of acetyl CoA, which gives rise to TCA cycle intermediates, can be calculated from the splitting pattern of glutamate resonances in the ^{13}C spectrum of heart extracts (29). The fraction of labeled acetyl CoA is equal to the doublet in the C-4 multiplet at 34.4 ppm multiplied by the ratio of total C-13 in glutamate C-4 to C-3 (27.9 ppm). This calculation does not depend on a steady state of the tracer metabolism.

RESULTS

Heart rate, arterial blood pressure, coronary sinus blood flow, and the high energy phosphates visible in ^{31}P-NMR spectra of the left ventricular apex were measured during venous infusions of 600 mM pyruvate or lactate into anesthetized intact dogs. Blood samples were drawn every 15 min from the coronary sinus and the carotid artery for measurements of glucose, lactate, pyruvate, alanine, and O_2, from which net myocardial extractions could be calculated. Because pyruvate or lactate infusion had the effect of raising arterial blood pH (4), the control level was intentionally set to <7.35. Although it was difficult to make an accurate measurement of intracellular pH from ^{31}P-NMR spectra in these experiments because of the changes in intracellular inorganic phosphate (P_i) concentration, intracellular pH did not appear to change (19). Increasing the plasma pyruvate past ~9 mM resulted in erratic heart beat and lowered pressures. Heart function immediately stabilized on withdrawal of the pyruvate infusion, and this correlated well with falling plasma pyruvate concentration. Arterial pH did not fall within this stabilization period and therefore did not correlate with heart function in these experiments.

Lactate and pyruvate extractions. Pyruvate extraction is reported in Table 1 at four plasma pyruvate concentrations between basal (0.13 mM) and 5.26 mM (*infusion period 3*), although the maximum concentration was higher in two experiments (Fig. 1). Pyruvate extraction was approximately linear with pyruvate concentration <3 mM, with an average initial slope of 0.154 ± 0.029 μmol/(mM plasma·min^{-1}·g wet wt^{-1}) (see Table 3). The entire data set can be linearized and fit to the Lineweaver-Burk

Table 1. *Pyruvate infusion*

	Control	Infusion Period		
		1	*2*	*3*
[Pyruvate], mM in plasma	0.13±0.027	0.86±0.033*	2.86±0.273*	5.26±0.408*
Range	0.07-0.20	0.79-0.92	2.45-3.61	4.11-5.86
Pyruvate extraction, μmol·min^{-1}·g wet wt^{-1}	0.018±0.008	0.139±0.037†	0.451±0.102†	0.581±0.067*
[Lactate], mM in blood	1.03±0.16	1.58±0.15†	3.00±0.39*	4.99±0.55*
Lactate extraction, μmol·min^{-1}·g wet wt^{-1}	0.068±0.024	0.134±0.030†	0.079±0.015	0.034±0.012
[Glucose], mM in blood	3.96±0.17	3.70±0.12	3.48±0.13	3.43±0.22
Glucose extraction, μmol·min^{-1}·g wet wt^{-1}	0.123±0.042	0.077±0.021	0.057±0.013	0.044±0.019
[Alanine], mM in plasma		0.79±0.12	0.88±0.18	1.01±0.15
Alanine extraction, μmol·min^{-1}·g wet wt^{-1}		−0.001±0.009	−0.020±0.011	−0.014±0.004
MVO_2, ml·min^{-1}·100 g^{-1}	3.39±0.64	3.70±0.69	3.94±0.92	3.26±0.62
Heart rate, min^{-1}	111±7	118±6	128±8	133±9
Mean pressure, mmHg	87±12	104±19	92±11	81±11
Coronary sinus blood flow	24±1	28±4	30±8	29±8
pH (arterial)	7.33±0.006	7.36±0.005*	7.42±0.022*	7.46±0.013*
pH (intracellular)	7.12±0.037	7.12±0.038	7.11±0.058	7.06±0.091
PCr/ATP	1.70±0	1.07±0.01†	1.15±0.04†	1.23±0.05†

Values are means ± SE, $n = 4$ for all values. Pyruvate and alanine are measured in plasma; lactate and glucose are measured in blood. Blood pyruvate concentration can be estimated by multiplying plasma pyruvate by (1 − hematocrit) = 0.63. MVO_2, mitochondrial respiration; PCr, phosphocreatine. * $P < 0.01$; † $P < 0.05$.

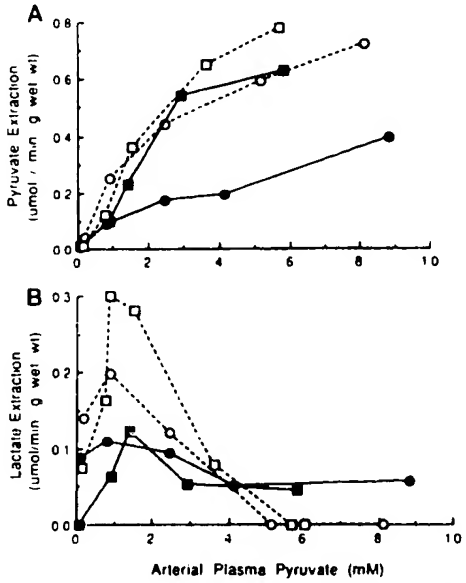

Fig. 1. Myocardial pyruvate extraction is plotted against arterial plasma pyruvate during a systemic infusion of pyruvate for each of 4 experiments (*A*). Lactate extraction is also shown as a function of plasma pyruvate (*B*).

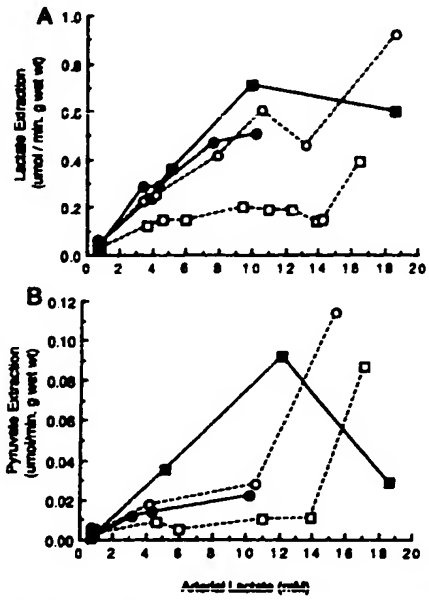

Fig. 2. Myocardial lactate extraction was measured during systemic lactate infusion and is plotted vs. arterial blood lactate (*A*). Pyruvate extraction was also measured in these animals (*B*).

equation. This yields an average correlation $r^2 = 0.982 \pm 0.025$. However, the V_{max} of 5.1 μmol·min^{-1}·g wet wt^{-1} and K_m of 39.4 mM plasma pyruvate estimated in this way are likely incorrect, since Eadie-Scatchard formalism yielded extremely nonlinear plots (40). Therefore, the extraction rates are thought to represent a composite of transport and intracellular phenomena and cannot easily be fit to first-order kinetic expressions.

Lactate concentration in blood increased linearly with pyruvate infusion, with an average slope of 0.69 ± 0.09 mM blood lactate/mM plasma pyruvate (see Table 3). When corrected for the hematocrit, this slope is ~1. Lactate extraction by the heart is normally linear with blood lactate concentration (see Refs. 12, 25, and Fig. 2), but in these experiments it increases only until plasma pyruvate reaches ~1 mM and then decreases toward zero with increasing plasma pyruvate (Table 1, Fig. 1*B*). At no point was either net pyruvate or lactate released by the heart.

During lactate infusion, lactate extraction increased with blood lactate concentration up to all concentrations achieved (2 experiments went to 25 mM). The data are summarized in Tables 2 and 3. Plasma pyruvate concentration increases approximately linearly with blood lactate, and pyruvate extraction was approximately linear with pyruvate concentration (Table 3). The slope was similar to the initial slope found when pyruvate was infused, indicating that although pyruvate inhibits lactate uptake, high arterial lactate seems to have little effect on pyruvate uptake. The ratio of the maximum slopes of pyruvate and lactate uptake (vs. the appropriate substrate) was 4–5 when corrected for hematocrit, indicating that under our conditions, pyruvate was transported and metabolized by the heart much more efficiently than lactate.

O_2 and glucose extraction did not change significantly during pyruvate or lactate infusion. Alanine is a direct product of pyruvate metabolism produced through transamination and can therefore be a route by which pyruvate is transported out of the cell without entry into the TCA cycle. During pyruvate infusion, alanine plasma concentration rose linearly with pyruvate but much more slowly. The total rate of alanine accumulation was only ~5% of the rate of increase in plasma pyruvate. Net myocardial alanine extraction was negative at elevated pyruvate concentrations, but the release of alanine never exceeded ~4% of pyruvate extraction. Lactate infusion did not alter alanine extraction.

High energy phosphates. The ^{31}P-NMR spectra were taken throughout the substrate infusions. Figure 3*C* shows a spectrum taken in the basal period (0.1 mM plasma pyruvate) and Fig. 3*B* at 8.8 mM plasma pyruvate. Figure 3*A* is the difference between the two, indicating the relative increase in PCr and decrease in the P_i region. The difference spectrum is complex in this region, since the intracellular P_i concentration falls with pyruvate infusion, and the extracellular P_i and blood 2,3-diphosphoglycerol have different chemical shifts due to an alkalinization of the blood with pyruvate infusion (6, 31). P_i was estimated to fall progressively to ≤50% of its control value by 6 mM plasma pyruvate. PCr/ATP does not change with lactate infusion until very high lactate levels are reached. The normalized values of PCr/ATP are given in Tables 1 and 2.

The chemical shift of β-ATP is sensitive to [Mg^{2+}], and it can be seen from the dispersive behavior in Fig. 3*A* that a change in intracellular free [Mg^{2+}] has occurred. Figure 4 shows that free [Mg^{2+}] fell during both pyruvate and lactate infusion. This is an important observation, since the K_{eq} for the many metabolic reactions, including the PCr kinase reaction and therefore the ratio PCr/ATP, is dependent on the [Mg^{2+}] (26). The values in Fig. 4 were calculated using an NMR equilibrium constant

Table 2. *Lactate infusion*

	Control	Infusion Period		
		1	*2*	*3*
[Lactate], mM in blood	0.78±0.06	4.31±0.07*	10.5±0.21*	17.5±1.1*
Range	0.67-0.89	4.17-4.50	10.2-11.1	15.3-18.6 (3)
Lactate extraction, μmol·min^{-1}·g wet wt^{-1}	0.037±0.007	0.24±0.037*	0.48±0.097†	0.56±0.19† (3)
[Pyruvate], mM in plasma	0.088±0.025	0.24±0.047†	0.51±0.18	0.75±0.24† (3)
Pyruvate extraction, μmol·min^{-1}·g wet wt^{-1}	0.003±0.001	0.020±0.006	0.038±0.019	0.077±0.024† (3)
[Glucose], mM in blood	3.77±0.14	3.78±0.10	3.90±0.08	3.76±0.27 (3)
Glucose extraction, μmol·min^{-1}·g wet wt^{-1}	0.082±0.028	0.045±0.005	0.065±0.016	0.037±0.023 (3)
[Alanine], mM in plasma		0.77±0.19 (3)	0.84±0.05 (3)	0.79±0.05 (3)
Alanine extraction, μmol·min^{-1}·g wet wt^{-1}		0.009±0.023 (3)	0.007±0.011 (3)	−0.052±0.017 (3)
$M\dot{V}O_2$, ml·min^{-1}·100 g^{-1}	2.15±0.47	1.93±0.26	2.28±0.55	2.35±0.48 (3)
Heart rate, min^{-1}	90±2	92±4	102±9	103±7 (3)
Mean pressure, mmHg	89±12	95±10	78±6	61±10 (3)
Coronary sinus blood flow, ml/min	16±2	18±5	21±5	20±4 (3)
pH (arterial)	7.32±0.012	7.36±0.013	7.38±0.011* (3)	7.40±0.009*
pH (intracellular)	7.15±0.008 (5)	7.16±0.017 (5)	7.14±0.33 (5)	7.09±0.097 (3)
PCr/ATP	1.00±0.01 (6)	1.00±0.02 (6)	1.08±0.03 (6)	1.12±0.04† (4)

Values are means ± SE; n = 4 unless otherwise indicated by nos. in parentheses. Pyruvate and alanine are measured in plasma; lactate and glucose are measured in blood. Blood pyruvate concentration can be estimated by multiplying plasma pyruvate by (1 − hematocrit) = 0.63. * $P < 0.01$; † $P < 0.05$.

[K_D(Mg-ATP)] of 0.045 mM (15). The absolute value for the calculated free [Mg^{2+}] is dependent on the choice of this constant, which varies a great deal in the literature. We chose this particular value because it yielded free Mg^{2+} concentrations that were similar to those estimated from the shift of citrate in the ^{13}C spectrum (5) of four of our experiments (2 in which [3-^{13}C]pyruvate was infused and 2 in which [3-^{13}C]lactate and unlabeled pyruvate were infused; see Figs. 6 and 7). The citrate chemical shifts gave an average of 778 ± 155 μM, which is similar to that found in perfused rat heart (850 ± 100 μM) using ^{19}F-NMR and fluorinated magnesium chelators (32). We can compare this with the values we obtained from the ATP chemical shift at 5.26 mM pyruvate (498 ± 30 μM) and 10.5 mM blood lactate (451 ± 27 μM). The disagreement of the ^{13}C-NMR citrate and the ^{31}P-NMR ATP measurements of magnesium is still significant, and its origin is unknown. However, the qualitative direction of the changes in free [Mg^{2+}] observed with pyruvate and lactate are reliable.

Table 3. *Regression data*

	Slope	y-Intercept	Correlation Coefficient
Pyruvate infusion			
Pyruvate extract vs. plasma pyruvate	0.154±0.029*	−0.020±0.012	0.962±0.009
Blood lactate vs. plasma pyruvate	0.69±0.09	1.02±0.16	0.990±0.004
Lactate infusion			
Lactate extract vs. blood lactate	0.053±0.010*†	0.036±0.028	0.971±0.011
Plasma pyruvate vs. blood lactate	[illegible]	[illegible]	[illegible]
Pyruvate extract vs. plasma pyruvate	0.07±0.025	0.001±0.002	0.861±0.090

Values are means ± SE, n = 4 for all analyses. Lactate is measured in whole blood, and pyruvate is measured in plasma. For direct comparisons, slopes measured vs. plasma pyruvate must be divided by 0.63. * Initial slope. † $P < 0.01$ vs. pyruvate extraction at elevated pyruvate

Carbon-13 NMR studies of lactate and pyruvate metabolism. The ^{13}C-NMR was used to determine the intracellular fate of extracted lactate and pyruvate. Dogs were prepared as for the ^{31}P-NMR experiments, except that a catheter was placed in the LAD for infusion of [3-^{13}C]pyruvate or [3-^{13}C]lactate. Figure 5*C* is a 22.5-min natural abundance ^{13}C-NMR spectrum of the dog heart in vivo. Figure 5*B* was taken between 45 and 67.5 min of an

[ADP] was calculated using the experimentally determined free [Mg^{2+}] and intracellular pH. Both [ADP] and free [Mg^{2+}] are shown in Fig. 4. It can be seen that [ADP] falls progressively to 75% of the control when pyruvate is infused but does not change significantly when lactate is the infused substrate, even though PCr/ATP tends to rise at the highest lactate concentration (Table 2).

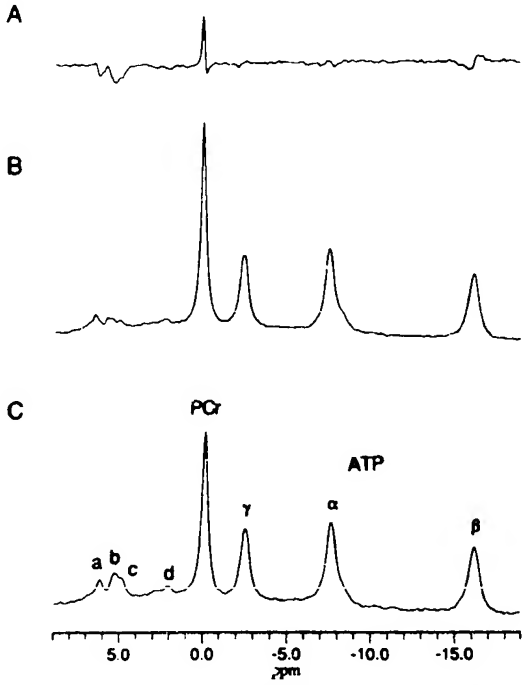

Fig. 3. Phosphorus-31 nuclear magnetic resonance (NMR) spectra taken of dog myocardium in vivo during infusion of sodium pyruvate. Each spectrum was taken in 24 min with a 2-s delay and was gated to respirator. Labeled resonances are α-, β-, and γ-ATP, phosphocreatine (PCr), 2,3-diphosphoglycerate (a), and 2,3-diphosphoglycerate and extracellular (b), intracellular inorganic phosphate (P_i; c), and phosphodiesters (d). *C*: taken during control period when arterial plasma pyruvate was 0.1 mM; *B*: accumulated at 8.8 mM plasma pyruvate. *A*: difference between the two, indicating relative rise in PCr and decrease in P_i and sugar phosphate regions. This region of spectrum is complex and represents both a loss of intracellular phosphate and a shift of the 2,3-diphosphoglycerate resonances due to changing arterial pH.

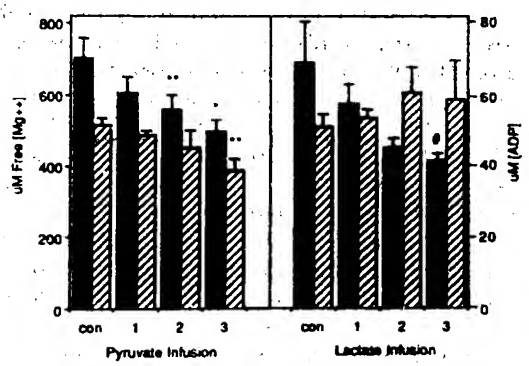

Fig. 4. Free intracellular $[Mg^{2+}]$ (solid bars) was calculated from ^{31}P-NMR chemical shifts of α- and β-ATP and an NMR dissociation constant of 0.045 mM (15). [ADP] (hatched bars) was then calculated using these $[Mg^{2+}]$ values and PCr/ATP and intracellular pH during each infusion period as defined in Tables 1 and 2. * $P < 0.05$ vs. control (con); ** $P < 0.01$ vs. control; # $P < 0.05$ vs. *period 1*.

infusion of 0.10 mmol/min [3-^{13}C]lactate, and Fig. 5*A* is the difference of the two. This infusion rate was meant to result in arterial label levels of between 6 and 16 mM in the region of the apex, dependent on the rate of LAD blood flow (averaged 10–12 ml/min whenever measured in similarly prepared dogs; see Ref. 25). The resulting peaks are lactate, alanine, and C-1 to C-4 of glutamate and glutamine (G-1 to G-4).

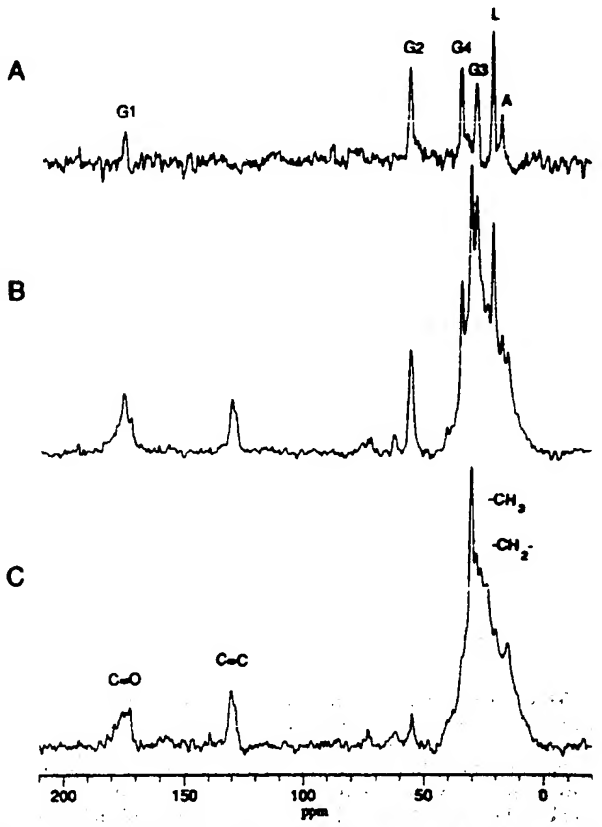

Fig. 5. Carbon-13 NMR spectra of a dog heart taken in vivo during control period (*C*) and during an infusion into left anterior descending artery (LAD) of 0.10 mmol/min [3-^{13}C]lactate (*B*). Each spectrum comprises 675 scans taken in 22.5 min with proton decoupling. Spectrometer was gated to respirator. In natural abundance spectra, methyl, double-bonded carbons, and carbonile carbons of fats are labeled. *A*: difference between the two is shown. Resonances are lactate (L), alanine (A), and glutamate plus glutamine C-1 to C-4 (G1 to G4).

After a control period during which natural abundance ^{13}C-NMR spectra were obtained, one of three infusion protocols was administered. In the first, [3-^{13}C]lactate was infused into the LAD at 0.10 mmol/min for 70 min (Fig. 6*B*). Figure 7 shows the resulting spectra from two experiments when 0.10 mmol/min of [3-^{13}C]pyruvate was infused. The third set (Fig. 6*A*) was conducted to determine whether lactate transport is affected by elevated pyruvate, which inhibits net lactate uptake. Plasma pyruvate was raised through a graded systemic infusion similar to that followed for ^{31}P-NMR experiments. When the difference between coronary-sinus and arterial blood lactate fell below its basal value (at an infusion rate of 0.9–1.05 mmol/min or ~5 mM plasma pyruvate), [3-^{13}C]-lactate was infused at 0.10 mmol/min for 45 min into the LAD. The systemic pyruvate infusion was maintained throughout the experiment.

When [3-^{13}C]lactate is the only infused substrate, the visible peaks are lactate in blood and tissue, intracellular alanine, and glutamate C-2 (55.5 ppm), C-3 (27.9 ppm), C-4 (34.4 ppm), and C-1 (174.9 ppm, shown on Fig. 5*A*). The glutamine resonances overlap the glutamate resonances except for C-4, which would appear at 31.4 ppm. We do not see a separate peak for C-4 glutamine, but it is possible that this is due to subtraction error in the large

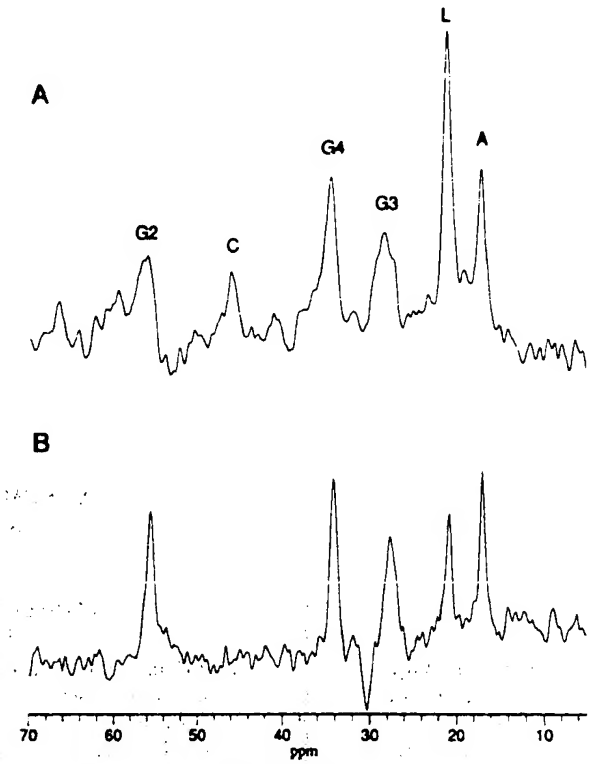

Fig. 6. Representative ^{13}C-NMR spectra of in vivo dog heart taken during a continuous infusion of 0.10 mmol/min [3-^{13}C]lactate into LAD. Each spectrum consists of 512 scans taken with 2-s delays with subtraction of a control. *A*: unlabeled pyruvate (1 mmol/min) was infused simultaneously into jugular vein. Labeled metabolites include alanine (A), lactate (L), glutamate and glutamine C-2 to C-4 (G2 to G4), and citrate (C). *B*: [3-^{13}C]lactate was only infused substrate

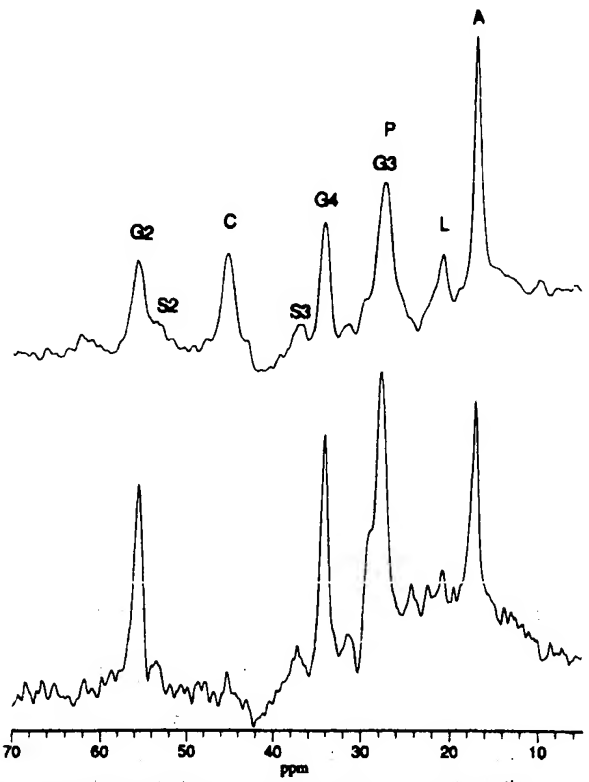

Fig. 7. Dog heart spectra from 2 experiments in which [3-^{13}C]pyruvate (0.10 mmol/min) was infused into LAD. Labeled metabolites are same as for Fig. 6. In addition, pyruvate (P) and aspartate C-2 and C-3 (S2, S3) are labeled. As can be seen, ^{13}C profiles taken in vivo varied a great deal between animals.

fat peak at this frequency. At 28.5 ppm, [3-^{13}C]pyruvate would appear, which cannot be resolved from the glutamate/glutamine C-3. This metabolite profile is somewhat different from that in the perfused heart in which only labeled glutamate is made from [3-^{13}C]lactate (41). It is possible that all the label is shuttled into glutamate in the perfused heart through the high activity of the malate-aspartate shuttle, which is needed to oxidize the NADH made from lactate (41). Because labeled alanine also appears in our spectra, this may indicate a lower shuttle activity with lactate in vivo than in perfused heart. When [3-^{13}C]pyruvate is the infused substrate (Fig. 7), the resultant in vivo spectra are very similar to those obtained in the perfused heart (41). Citrate C-2 appears at 46.5 ppm, and small aspartate peaks can be seen at 37.5 ppm and 53.1 ppm. The [3-^{13}C]lactate peak is very small; out of four dogs, the one shown in Fig. 7, *top*, had by far the largest lactate peak. When unlabeled pyruvate and [3-^{13}C]lactate were infused together (Fig. 6*A*), citrate C-2 is visible, similar to when [3-^{13}C]pyruvate is the sole substrate. Under these conditions, however, the lactate-to-alanine ratio is high, perhaps partly due to a contribution from blood [3-^{13}C]lactate. The glutamate signal-to-noise ratio is much lower than when [3-^{13}C]-lactate is the sole infused substrate, reflecting the reduced enrichment of intracellular compounds and a lower total glutamate concentration (Table 4, Ref. 41).

The average time course of the signals measured in vivo

Table 4. *Enrichment of lactate, alanine, and acetyl-CoA with ^{13}C in heart extracts*

Infusion	Measured Enrichment		Calculated Enrichment for Acetyl-CoA
	Alanine	Lactate	
[3-^{13}C]lactate	0.53±0.05	0.59±0.04	0.57±0.04
[3-^{13}C]pyruvate	0.41±0.09	0.23±0.01	0.38±0.09
[3-^{13}C]lactate + systemic pyruvate	0.37±0.05	0.41±0.06	0.36±0.08

Values are means ± SE, $n = 3$ for each group. Infusions were into left anterior descending artery unless otherwise indicated. Alanine and lactate enrichment were measured in ^{1}H-nuclear magnetic resonance (NMR) spectra of heart extracts. Acetyl-CoA enrichments were calculated from the splitting pattern of glutamate resonances in ^{13}C-NMR spectra of heart extracts (29).

are shown in Fig. 8, *A* and *B*, for lactate infused into four dogs. The areas of all peaks are normalized to alanine. Lactate and alanine reach a steady state by 25 min, and glutamate (plus glutamine) C-4 reached steady state by 35 min. Incorporation of label into glutamate plus glutamine C-3 and C-4 continued as their intensities approached that of C-4. Four additional dogs were infused at the same rate with [3-^{13}C]pyruvate. The time course for the experiment shown in Fig. 7, *top*, is shown in Fig. 9, *A* and *B*. Alanine, lactate, and citrate all reach a steady state within 25 min. Glutamate plus glutamine C-4 reaches its steady state by ~30 min, and C-2 and C-3 approach steady state near 60 min, as with lactate infusion. The

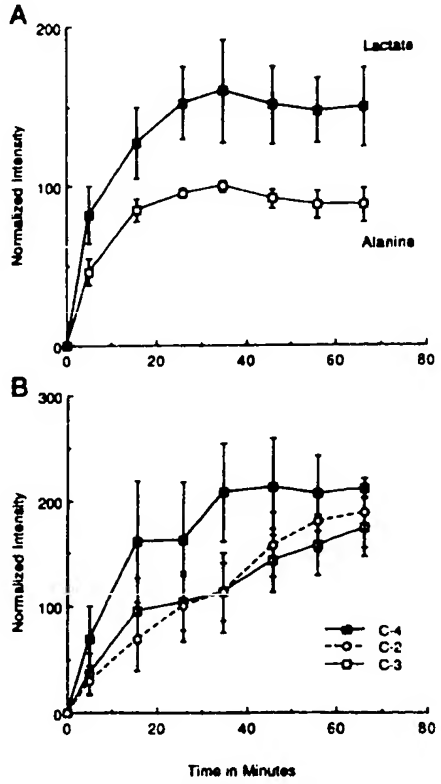

Fig. 8. Average time courses of labeled compounds seen in vivo in ^{13}C-NMR spectra of dog heart during infusion of 0.10 mmol/min [3-^{13}C]-lactate (n = 4 dogs). Peak areas were measured in 10-min spectra and plotted at midpoint time. *A*: [3-^{13}C]lactate and [3-^{13}C]alanine signals, which reach steady-state values by 25 min. *B*: ^{13}C at glutamate and glutamine C-2, C-3, and C-4. C-4 reaches a steady-state enrichment by ~35 min, but C-2 and C-3 continue to increase throughout experiment.

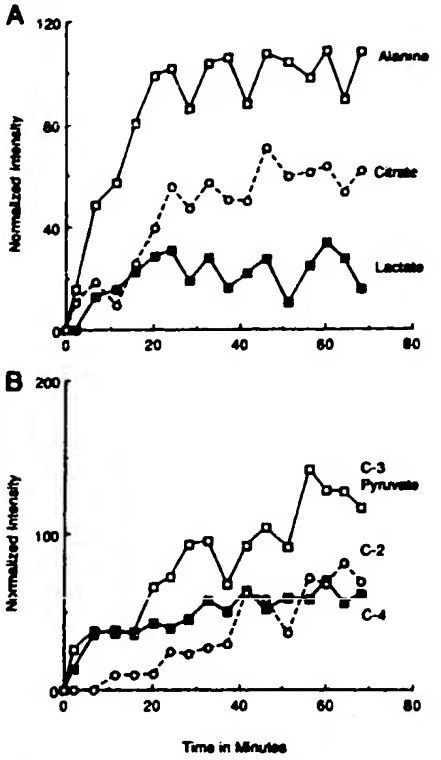

Fig. 9. Representative set of time courses taken during [3-^{13}C]pyruvate infusion (0.1 mmol/min). Compounds are same as in Fig. 8, except that citrate is included. Time to steady state is similar to lactate infusion for alanine, citrate, and small lactate peak (*A*). *B*: glutamate and glutamine C-4 also have a similar time course to that seen when [3-^{13}C]lactate is substrate. C-2 and C-3 reach their steady-state areas by ~60 min. Difference between C-3-glutamate plus pyruvate and C-2-glutamate peak areas is intra- plus extracellular pyruvate, which presumably follows a time course similar to alanine.

resonance at 28 ppm includes plasma pyruvate as well as C-3 glutamate and glutamine and is therefore the sum of at least two curves, one of which has a time constant similar to alanine and one similar to C-2 glutamate plus glutamine. Subtraction of the C-2 curve from the C-3 plus pyruvate curve yields an area for the steady state pyruvate of 55% of alanine in this animal. The results in vivo during infusion of labeled pyruvate are quite variable. Glutamate C-2, C-3, and C-4 are present in all four animals, alanine was visible in 3, and a small resonance for lactate could be seen in only one (shown in Fig. 7).

The enrichment with ^{13}C was determined for alanine and lactate in proton NMR spectra of extracts of heart tissue freeze clamped at the end of the ^{13}C-NMR experiment. An example of a proton spectrum of a heart extract from a dog infused with [3-^{13}C]lactate and unlabeled pyruvate is shown in Fig. 10, and the results are reported in Table 4 (n = 3 for each group). In theory, the same measurement can be made for glutamate, but in practice these resonances are convoluted with those from glutamine and difficult to decipher. Malloy et al. (29) have shown that the labeling pattern of C-3 and C-4 of glutamate in ^{13}C-NMR spectra of extracts (Fig. 11) can be used to calculate the ^{13}C enrichment of acetyl CoA entering the TCA cycle under non-steady-state conditions. The acetyl CoA enrichment is equal to the area of the doublet in the C-4 multiplet at 34.4 ppm multiplied by the ratio of total ^{13}C at C-4 to that at C-3. Alanine is thought to be in steady state with pyruvate; if so, the two metabolite pools would have the same ^{13}C enrichment. As can be seen in Table 4, the enrichment of alanine is always equal to the calculated acetyl CoA enrichment. This is evidence that alanine and pyruvate do have similar enrichments and that oxidation of other substrates that enter the TCA cycle as acetyl CoA (fatty acids or ketone bodies) is minimal when either lactate or pyruvate concentrations are high. This supports the observed ability of lactate to inhibit fatty acid oxidation in hearts of intact dogs (7, 42). The lactate enrichment is much lower than alanine enrichment when the label is infused as pyruvate, indicating that under these conditions the pyruvate pool is likely to be in equilibrium with alanine but not with cellular lactate. The low lactate ^{13}C enrichment in the heart extracts explains why the [3-^{13}C]lactate signal is low in the heart in vivo during [3-^{13}C]pyruvate infusion.

Lactate and pyruvate are in constant exchange in the body, which makes whole body studies of lactate metabolism by tracers very difficult (27, 49). Blood and heart tissue both act as mediators of this exchange (11, 13). To examine whether ^{13}C exchange occurs between blood pyruvate and lactate during the short transit time from the LAD infusion point to the apex where the NMR

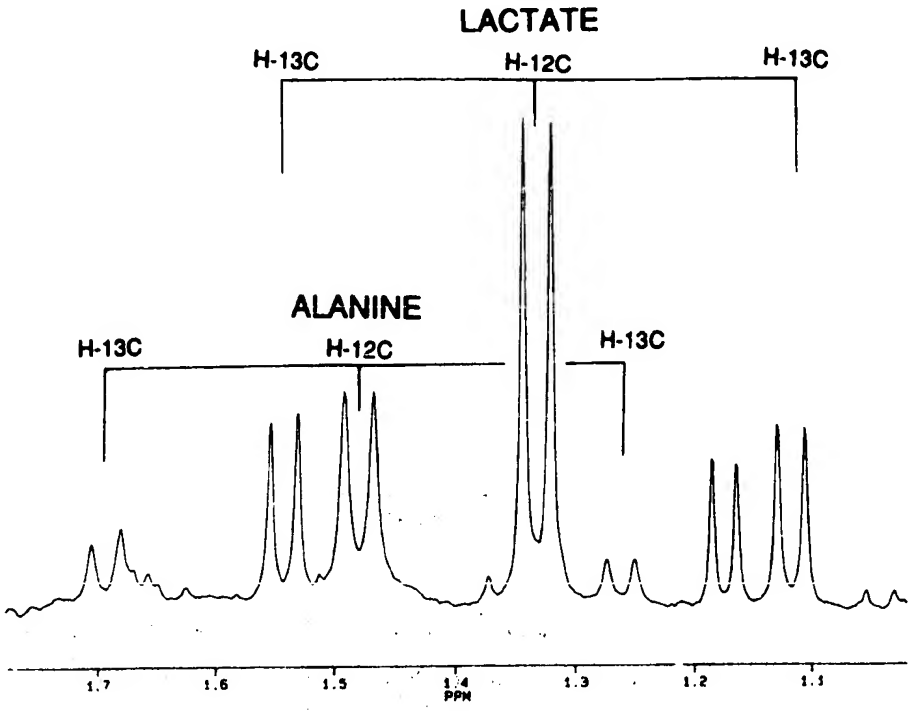

Fig. 10. Methyl region of proton spectrum of a perchloric acid extract of heart taken at 300 MHz, which consists of 64 scans, 90° pulses, and 10-s interpulse delays. Dog was infused intravenously with 1 mmol/min unlabeled pyruvate and in LAD with 0.10 mmol/min [3-^{13}C]lactate. Unlabeled lactate methyl protons resonate at 1.33 ppm, and methyl protons of [3-^{13}C]lactate are split with a J coupling constant of 128 Hz. Unlabeled alanine methyl protons are found at 1.48 ppm, and [3-^{13}C]alanine methyl protons also show a J coupling of 128 Hz. Enrichment is ratio of 2 H-^{13}C peaks to total area (H-^{13}C + H-^{12}C).

spectrum is taken, a catheter was placed on the surface of the heart in the venous return from the apex. Venous blood was sampled at 15 and 30 min of an LAD infusion of 0.10 mmol/min each of [3-^{13}C]lactate and unlabeled pyruvate in two dogs. The hearts were freeze clamped immediately thereafter. At 15 min, the enrichment of blood lactate was 64 ± 7% (5.7 ± 0.4 mM total) and that of blood pyruvate was 17 ± 5% (4.2 ± 0.1 mM total). At 30 min, blood lactate enrichment was 66 ± 12% (5.6 ± 0.1 mM total) and blood pyruvate was 18 ± 7% (4.3 ± 0.7 mM total). The error is expressed as SD between the two experiments. Therefore, considerable flux of label occurs between blood lactate and pyruvate in the short distance between the LAD and the venous return from the apex, and the ^{13}C peaks measured in vivo may have contributions of label from both. However, the label most likely traces the metabolic pattern due to the dominant substrate (Figs. 6 and 7). Alanine ^{13}C enrichment in the freeze-clamped hearts from these two experiments was 34 ± 4%, which is similar to that measured in the related experiments in the third row of Table 4. This is well over the enrichment of blood pyruvate, indicating that an appreciable amount of the label in these hearts comes from blood lactate. Pyruvate at these concentrations inhibits net lactate uptake (Table 1, Fig. 1), but these results show that the flux of lactate across the membrane and into the intracellular pyruvate pool is maintained.

DISCUSSION

There are several major observations in this study. The first is that similar to the perfused heart, the phosphorylation potential (ATP/ADP × P_i) of the myocardium was elevated during pyruvate infusion in vivo but not during lactate infusion. This is especially surprising,

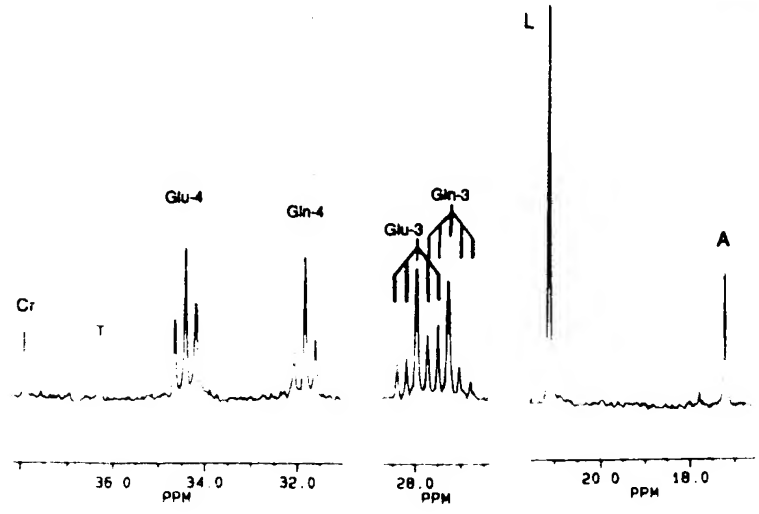

Fig. 11. Proton-decoupled ^{13}C-NMR spectrum taken at 75.47 MHz of perchloric acid extract of heart infused only with [3-^{13}C]lactate (0.1 mmol/min into LAD). This spectrum was acquired with 90° pulse and 20-s interpulse delay without nuclear Overhauser effect development. Splitting pattern of glutamate C-3 and C-4 peaks was used to calculate ^{13}C enrichment of acetyl CoA entering TCA cycle by method of Malloy et al. (29). Labeled resonances are natural abundance creatine (Cr) and taurine (T), and ^{13}C-labeled glutamate (Glu-3 and 4), glutamine (Gln-3 and 4), lactate (L), and alanine (A).

since both compounds share a common metabolic fate. The second observation is that the elevated pyruvate prevented net lactate uptake, although no significant effect of lactate was observed on pyruvate extraction. Third, intracellular lactate and pyruvate were in equilibrium during lactate infusion but not when pyruvate was the substrate. Evidence for this is the small or absent [3-^{13}C]-lactate peak in the spectra taken in vivo during [3-^{13}C]-pyruvate infusion, at least partially due to the fact that intracellular lactate enrichment was only one-half that of pyruvate under these conditions.

Unfortunately, it was difficult to quantitate changes in intracellular P_i and therefore to precisely calculate the ratio ATP/ADP × P_i. However, [ADP] could be calculated from PCr/ATP and the intracellular free magnesium ion (Fig. 4; Refs. 15, 26). [ADP] fell by 25% at the highest pyruvate infusion, indicating that the change in phosphorylation potential was at least as large. The small rise in PCr/ATP seen with lactate infusion was offset by a fall in free [Mg^{2+}], and the calculated [ADP] was unchanged from control. These differences in phosphorylation potential are unrelated to O_2 extraction or heart work, which were essentially unchanged by either infusion. There are two sites where lactate and pyruvate may differ in their ability to change the phosphorylation potential: the mitochondrial redox state (24) or cytoplasmic NADH/NAD^+ (30, 46, 47). We and others (33; F. Heineman and T. Scholz, unpublished results) have found using surface fluorescence that the mitochondria are reduced to the same extent in perfused heart with either pyruvate or lactate as substrate. The difference in phosphorylation potential is therefore most likely linked to the action of the LDH equilibrium on the cytosolic redox potential. When pyruvate is converted to lactate, NADH is converted to NAD^+, resulting in an overall oxidation of the cell (48). The redox state may in turn be linked to the high energy phosphate ratio through the action of the abundant glycolytic enzymes 3-phosphoglycerate kinase and glyceraldehyde-3-phosphate dehydrogenase, which have a combined K_{eq} of 59 at neutral pH (30, 46, 47). A decrease in NADH/NAD^+ would be expected to raise ATP/ADP × P_i. Kingsley-Hickman et al. (22) have used ^{31}P-NMR saturation transfer techniques to estimate that the unidirectional rate of cytosolic ATP synthesis in glucose-perfused heart is 4.0 $\mu mol \cdot s^{-1} \cdot g$ dry wt^{-1} or ~15 times the maximal glycolytic flux, indicating that the activity of the cytoplasmic dehydrogenase-linked ATP synthase is high enough to keep its substrates in equilibrium.

Why doesn't the phosphorylation potential fall with lactate infusion, which would be expected to increase the NADH/NAD^+ ratio in the heart cytoplasm? The answer is unknown, but one could speculate that the redox state actually changes very little, either because increased lactate uptake is always accompanied by increased pyruvate uptake or because of the high activity of the malate aspartate and α-glycerophosphate shuttles that transport the cytosolic NADH produced during lactate metabolism into the mitochondria (39).

We can address the first suggestion with reference to Tables 1 and 2. When plasma pyruvate was raised to 5.3 mM, net lactate uptake was inhibited, and the ratio of extracted lactate/pyruvate fell to <2% of basal (Table 1). This is consistent with decreased intracellular [lactate]/[pyruvate] and oxidation of the cytoplasm. Conversely, the ratio of extracted lactate to pyruvate remained stable as blood lactate was raised. When lactate reached 17.5 mM, the extracted lactate/pyruvate actually fell from 12 to 7 (Table 2). If the intracellular [lactate]/[pyruvate] parallels the ratio of uptake of these compounds, the redox potential would not be expected to change appreciably during lactate infusion.

The malate-aspartate shuttle is known to be very active in the perfused heart. The importance of this shuttle has been demonstrated with specific inhibitors. When aspartate transaminase, a key enzyme in the shuttle, is inhibited by amino-oxyacetate in lactate-perfused heart, NADH/NAD^+ rises dramatically (39). Thus, during lactate infusion in vivo, a rise in NADH/NAD^+ may be minimized by the malate-aspartate shuttle. Kobayashi and Neely (23) suggest that lactate and glucose metabolism are ultimately limited by the rate at which cytosolic NADH is replaced by NAD^+ through this shuttle. This shuttle may also explain why [3-^{13}C]lactate as the sole substrate gives rise primarily to labeled glutamate in the perfused heart, whereas [3-^{13}C]pyruvate also results in labeled alanine, citrate, and aspartate. Sherry et al. (41) suggested that the TCA cycle intermediates are drained into the glutamate pool as NADH produced during lactate metabolism is shuttled into the mitochondria.

Our second observation is that although lactate and pyruvate extraction were both functions of circulating concentration, the fractional extraction of lactate was less than for pyruvate, and lactate extraction was attenuated at high pyruvate concentrations. There are data in the literature in support of several potential mechanisms for this inhibition of net lactate uptake. Pyruvate may competitively inhibit lactate transport at the cell membrane (18, 37, 44, 45), balance lactate extraction with production from pyruvate through simple mass action (10), or inhibit LDH, preventing lactate from entering the pyruvate pool (8).

It has been demonstrated in cardiac sarcolemmal vesicles that pyruvate and lactate are transported by the same pH-dependent monocarboxylate carrier (44, 45). Both are transported with a proton so that flux is accelerated by a pH gradient toward the lower H^+ concentration. The K_m for transport is much lower than that for lactate, and this has been measured in sarcolemmal vesicles (4.0 mM for pyruvate vs. >27 mM for lactate; see Refs. 44, 45), isolated cardiac myocytes (<0.1 mM vs. 2.3 mM for L-lactate; see Ref. 37), and in perfused heart, where the efflux of pyruvate as a function of its intracellular concentration is 15 times greater than the efflux of lactate (18). Excess pyruvate has been shown to be a competitive inhibitor of L-lactate transport (44, 45). However, the data in Table 4 do not support limited transport as a mechanism for inhibition of lactate uptake. When [3-^{13}C]lactate is the only substrate infused, heart lactate, alanine, and acetyl CoA pools have the same specific activity. When [3-^{13}C]lactate and unlabeled pyruvate were infused together, net lactate uptake was low.

However, the specific activity of alanine and acetyl CoA were similar to when [3-^{13}C]pyruvate was the sole infused substrate, indicating appreciable lactate transport. Finally, the enrichment of lactate lags behind that of alanine and acetyl CoA when [3-^{13}C]pyruvate is the substrate, which shows that transport of unlabeled lactate across the membrane into the intracellular pool is fast compared with the flux of pyruvate to lactate under these conditions. This lack of LDH flux would explain why very little [3-^{13}C]lactate is produced in the carbon spectra taken in vivo during [3-^{13}C]pyruvate infusion.These data suggest that LDH-driven flux between the intracellular lactate and pyruvate pools is fast under conditions where lactate alone or lactate and pyruvate are elevated together and slow (relative to lactate transport) when pyruvate is raised alone. Although usually thought of as an unregulated, near-equilibrium enzyme, it has been predicted that H-type LDH (78% of that found in heart) could be inhibited in vivo. In studies of the isolated enzyme, a dead-end pyruvate-NAD^+ complex slowly forms at physiological concentrations of pyruvate and NAD^+. This inhibition is immediately reversed when either lactate or NADH are added in vitro (8). LDH may therefore be inhibited by elevated pyruvate in vivo, yet coinfusion of [3-^{13}C]lactate (arterial levels between 6 and 16 mM) would raise the intracellular lactate enough to overcome this inhibition. Our data support the conclusion that myocardial LDH is a regulated enzyme with reduced activity in the presence of elevated pyruvate.

In summary, the extraction, intracellular carbon, and high energy phosphate metabolism of lactate and pyruvate were measured in vivo in the dog heart. Pyruvate fractional extraction exceeded that of lactate by a factor of 5, and elevated pyruvate severely reduced the net uptake of lactate but not its transport into the cell. Pyruvate also inhibits myocardial LDH, and lactate relieves this inhibition. Both substrates suppress oxidation of other molecules and cause intracellular free [Mg^{2+}] to fall but do not alter work output or O_2 extraction. Pyruvate, but not lactate, results in a decrease in [ADP] and an elevated phosphorylation potential. The change in phosphorylation potential is therefore due to a cytosolic event, most likely the redox state. These data indicate that the phosphorylation potential of the heart is a function of the cytosolic as well as mitochondrial energy state, and that this can be manipulated in vivo by choice of substrate.

Address for reprint requests: M. R. Laughlin, Laboratory of Cardiac Energetics, National Heart, Lung, and Blood Institute, National Institutes of Health, 9000 Rockville Pike, Bldg. 1, Rm. B3-07, Bethesda, MD 20892.

Received 15 May 1992; accepted in final form 10 December 1992.

REFERENCES

1. **Bertrand, M. E., A. G. Carre, A. P. Ginestet, J. M. Lefebvre, L. A. Desplanque, and L. P. Lekiefre.** Maximal exercise in normal subjects. Changes in coronary sinus blood flow, contractility and myocardial extraction of FFA and lactate. *Eur J Cardiol* 5/6: 481-491, 1977.

Bucher, T., R. Czok, W. Lamprecht, and E. Latzko. Pyruvate. In: *Methods of Enzymatic Analysis*, edited by H. U. Bergmeyer. New York: Academic, 1963, p. 253-259.

3. **Bunger, R., R. T. Mallet, and D. A. Hartman.** Pyruvate-enhanced phosphorylation potential and inotropism in normoxic and postischemic isolated working heart. *Eur J. Biochem* 180: 221-223, 1989.

4. **Cohen, R. D., R. A. Iles, D. Burnett, M. E. O. Howell, and J. Strunin.** The effect of changes in lactate uptake on the intracellular pH of the perfused rat liver. *Clin. Sci. Lond.* 41: 159-170, 1971.

5. **Cohen, S. M.** Simultaneous ^{13}C and ^{31}P NMR studies of perfused rat liver. *J. Biol. Chem.* 258: 14294-14308, 1983.

6. **Costello, A. J. R., W. E. Marshall, A. Omachi, and T. O. Henderson.** Interactions between hemoglobin and organic phosphates investigated with ^{31}P magnetic resonance spectroscopy and ultrafiltration. *Biochim. Biophys. Acta* 427: 481-491, 1976.

7. **Drake, A. J., J. R. Haines, and M. I. M. Noble.** Preferential uptake of lactate by the normal myocardium in dogs. *Cardiovasc. Res.* 14: 65-72, 1980.

8. **Everse, J., and N. O. Kaplan.** Lactate dehydrogenase: structure and function. *Adv. Enzymol. Relat. Areas Mol. Biol.* 37: 61-133, 1973.

9. **From, A. H., S. D. Zimmer, S. P. Michurski, P. Mohanadrishnan, V. K. Ulstad, W. J. Thoma, and K. Ugurbil.** Regulation of the oxidative phosphorylation rate in the intact cell. *Biochemistry* 29: 3731-3743, 1990.

10. **Garland, P. B., E. A. Newsholme, and P. J. Randle.** Regulation of glucose uptake by muscle. *Biochem. J.* 93: 665-667, 1964.

11. **Gertz, E. W., J. A. Wisneski, R. A. Neese, J. D. Bristow, G. L. Searle, and J. T. Hanlon.** Myocardial lactate metabolism: evidence for lactate release during net chemical extraction in man. *Circulation* 63: 1273-1279, 1981.

12. **Gertz, E. W., J. A, Wisneski, R. Neese, A. Houser, R. Korte, and J. D. Bristow.** Myocardial lactate extraction: multidetermined metabolic function. *Circulation* 61: 256-261, 1980.

13. **Halestrap, A. P., R. C. Poole, and S. L. Cranmer.** Mechanisms and regulation of lactate, pyruvate and ketone body transport across the plasma membrane of mammalian cells and their metabolic consequences. *Biochem. Soc. Trans.* 18: 1132-1135, 1990.

14. **Hassinen, I., I. Kinji, S. Nioka, and B. Chance.** Mechanism of fatty acid effect on myocardial oxygen consumption. A phosphorus NMR study. *Biochim. Biophys. Acta* 1019: 73-80, 1990.

15. **Headrick, J. P., and R. J. Willis.** Effect of inotropic stimulation on cytosolic Mg^{2+} in isolated rat heart: a ^{31}P magnetic resonance study. *Magn. Reson. Med.* 12: 328-338, 1989.

16. **Heineman, F. W., and R. S. Balaban.** Phosphorus-31 nuclear magnetic resonance analysis of transient changes of canine myocardial metabolism in vivo. *J. Clin. Invest.* 85: 843-852, 1990.

17. **Heineman, F. W., and R. S. Balaban.** Control of myocardial oxygen consumption by work. In: *The Heart and Cardiovascular System* (2nd ed.), edited by H. A. Fozzard. New York: Raven, 1992, p. 1641-1656.

18. **Henderson, A. H., R. J. Craig, R. Gorlin, and E. H. Sonnenblick.** Lactate and pyruvate kinetics in isolated perfused rat hearts. *Am. J. Physiol.* 217: 1752-1756, 1969.

19. **Katz, L. A., J. A. Swain, M. A. Portman, and R. S. Balaban.** Intracellular pH and inorganic phosphate content of heart in vivo: a ^{31}P-NMR study. *Am. J. Physiol.* 255 (*Heart Circ Physiol.* 24): H189-H196, 1988.

20. **Keul, J.** Myocardial metabolism in athletes. *Adv. Exp. Med. Biol.* 11: 447-467, 1971.

21. **Kim, D. K., F. W. Heineman, and R. S. Balaban.** Effects of β-hydroxybutyrate on oxidative metabolism and phosphorylation potential in canine heart in vivo. *Am. J. Physiol.* 260 (*Heart Circ. Physiol.* 29): H1767-H1772, 1991.

22. **Kingsley-Hickman, P. B., E. Y. Sako, P. Mohanakrishnan, P. M. L. Robitaille, A. H. L. From, J. E. Foker, and K. Ugurbil.** ^{31}P-NMR studies of ATP synthesis and hydrolysis kinetics in the intact myocardium. *Biochemistry* 26: 7501-7510, 1987.

23. **Kobayashi, K., and J. R. Neely.** Control of maximum rates of glycolysis in rat cardiac muscle *Circ Res* 44: 166-175, 1979.

Koretsky, A. P., and R. S. Balaban. Changes in pyridine nucleotide levels alter oxygen consumption and extra-mitochondrial phosphates in isolated mitochondria: a ^{31}P-NMR and fluorescence study. *Biochim. Biophys. Acta* 893: 398-408, 1987.

25. **Laughlin, M. R., J. F. Taylor, A. S. Chesnick, and R. S. Balaban.** Regulation of glycogen metabolism in canine myocardium: effects of insulin and epinephrine in vivo. *Am. J. Physiol.* 262 (*Endocrinol. Metab.* 25): E875-E883, 1992.

26. **Lawson, J. W. R., and R. L. Veech.** Effects of pH and free Mg^{2+} on the K_{eq} of the creatine kinase reaction and other phosphate hydrolyses and phosphate transfer reactions. *J. Biol. Chem.* 254: 6528-6537, 1979.
27. **Lehman, S. L.** Measurement of lactate production by tracer techniques. *Med. Sci. Sports Exercise* 23: 935-938, 1991.
28. **Mallet, R. T., D. A. Hartman, and R. Bunger.** Glucose requirement for postischemic recovery of perfused working heart. *Eur. J. Biochem.* 188: 481-493, 1990.
29. **Malloy, C. R., J. R. Thompson, F. M. H. Jeffrey, and A. D. Sherry.** Contribution of exogenous substrates to acetyl coenzyme A: measurement by ^{13}C-NMR under non-steady-state conditions. *Biochemistry* 29: 6756-6761, 1990.
30. **Masuda, T., G. P. Dobson, and R. L. Veech.** The Gibbs-Donnan near-equilibrium system of heart. *J. Biol. Chem.* 265: 20321-20334, 1990.
31. **Moon, R. B., and J. H. Richard.** Determination of intracellular pH by ^{31}P magnetic resonance. *J. Biol. Chem.* 248: 7276-7278, 1973.
32. **Murphy, E., C. Steenbergen, L. A. Levy, B. Raju, and R. E. London.** Cytosolic free magnesium levels in ischemic rat heart. *J. Biol. Chem.* 264: 5622-5627, 1989.
33. **Nuutinen, E. M.** Subcellular origin of the surface fluorescence of reduced nicotinamide nucleotides in the isolated perfused rat heart. *Basic Res. Cardiol.* 79: 49-58, 1984.
34. **Peuhkurinen, K. J., and I. E. Hassinen.** Pyruvate carboxylation as an anaplerotic mechanism in the isolated perfused rat heart. *Biochem. J.* 202: 67-76, 1982.
35. **Peuhkurinen, K. J., J. K. Hiltunen, and I. E. Hassinen.** Metabolic compartmentation of pyruvate in the isolated perfused rat heart. *Biochem. J.* 210: 193-198, 1983.
36. **Pfleiderer, G.** L-Alanine, determination with glutamate-pyruvate transaminase and lactic dehydrogenase. In: *Methods of Enzymatic Analysis*, edited by H. U. Bergmeyer. New York: Academic, 1963, p. 378-380.
37. **Poole, R. C., Halestrap, A. P., S. J. Price, and A. J. Levi.** The kinetics of transport of lactate and pyruvate into isolated cardiac myocytes from guinea pig. *Biochem. J.* 264: 409-418, 1989.
38. **Randle, P. J., and P. K. Tubbs.** Carbohydrate and fatty acid metabolism. *Handbook of Physiology. The Cardiovascular System.* Bethesda, MD: Am. Physiol. Soc., 1977, sect. 2, vol. I, chapt. 23, p. 805-844.
39. **Safer, B., C. M. Smith, and J. R. Williamson.** Control of the transport of reducing equivalents across the mitochondrial membrane in perfused rat heart. *J. Mol. Cell. Cardiol.* 2: 111-124, 1971.
40. **Segal, I. H.** *Enzyme Kinetics: Behavior and Analysis of Rapid Equilibrium and Steady-State Enzyme Systems.* New York: Wiley, 1975, p. 214-218.
41. **Sherry, A. D., R. L. Nunnally, and M. R. M. Peshock.** Metabolic studies of pyruvate- and lactate-perfused guinea pig hearts by ^{13}C-NMR. *J. Biol. Chem.* 260: 9272-9279, 1985.
42. **Spitzer, J. J.** Effect of lactate infusion on canine myocardial FFA metabolism in vivo. *Am. J. Physiol.* 226: 213-217, 1974.
43. **Starnes, J. W., D. F. Wilson, and M. Erecinska.** Substrate dependence of metabolic state and coronary flow in perfused rat heart. *Am. J. Physiol.* 249 (*Heart Circ. Physiol.* 18): H779-H806, 1985.
44. **Trosper, T. L., and K. D. Philipson.** Lactate transport by cardiac sarcolemmal vesicles. *Am. J. Physiol.* 252 (*Cell Physiol.* 21): C483-C489, 1987.
45. **Trosper, T. L., and K. D. Philipson.** Functional characteristics of the cardiac sarcolemmal monocarboxylate transporter. *J. Membr. Biol.* 112: 15-23, 1989.
46. **Veech, R. L., J. W. R. Lawson, N. W. Cornell, and H. A. Krebs.** Cytosolic phosphorylation potential. *J. Biol. Chem.* 254: 6538-6547, 1979.
47. **Veech, R. L., L. Raijman, and H. A. Krebs.** Equilibrium relations between the cytoplasmic adenine nucleotide system and nicotinamide-adenine nucleotide system in rat liver. *Biochem. J.* 117: 499-503, 1970.
48. **Williamson, J. R.** Glycolytic control mechanisms. *J. Biol. Chem.* 240: 2308-2321, 1965.
49. **Wolfe, R. R., F. Jahoor, and H. Miyoshi.** Evaluation of the isotopic equilibrium between lactate and pyruvate. *Am. J. Physiol.* 254 (*Endocrinol. Metab.* 17): E532-E535, 1988.
50. **Zweier, J. L., and W. E. Jacobus.** Substrate-induced alterations of high-energy phosphate metabolism and contractile function in the perfused heart. *J. Biol. Chem.* 262: 8015-8021, 1987.